Indian Journal of Engineering & Materials Sciences
Vol. 27, April 2020, pp. 309-319

Machining performance enhancement of EN-31 diesteel using MWCNT mixed rotary EDM

Rajesh Bajaj[a,b*], Amit Rai Dixit[c], Arun Kumar Tiwari[d] & Nitin Kumar Chauhan[e]

[a,b,c]Department of Mechanical Engineering, Indian Institute of Technology (ISM), Dhanbad 826004, India
[d]Department of Mechanical Engineering, Institute of Engineering and Technology, Lucknow 226021, India
[e]Department of Mechanical Engineering, JSS Academy of Technical Education, Noida 201301, India

Received: 05 November 2018 ; Accepted: 26 July 2019

The present study investigates the influence of adding multi-wall carbon nanotube (MWCNT) into the dielectric fluid of electric discharge machining (EDM) in terms of material removal rate (MRR), surface roughness (SR) and surface topology of EN-31 die steel using Cu electrode. A customized rotary electrode set-up has been developed to compare the performance improvement of powder mixed rotary electrical discharge machining (PMREDM) as compared to powder mixed electrical discharge machining (PMEDM) and conventional EDM. The present study attempts to investigate the optimization of process parameters of MWCNT mixed rotary EDM of EN-31 die steel using response surface methodology (RSM) and genetic algorithm (GA) in terms of MRR and SR. The optimization results show that MWCNT mixed rotary EDM shows highest value of MRR (9.72 mm^3/min) and lowest value of SR (R_a = 2.03 µm), which are approximately 46.17% higher and 45.43% lower than conventional EDM values respectively. Further, various combinations of optimal values of MRR and SR and their corresponding input parameters setting have been shown in pareto table created by multi-objective optimization GA technique available in *MATLAB*. Finally, field emission scanning electron microscope (FESEM) analysis of MWCNT mixed rotary EDM and EDM surfaces is carried out which revealsthat MWCNT mixed rotary EDM shows better surface topography as compared to EDM process.

Keywords: Material removal rate, Surface roughness, Genetic algorithm, Powder mixed electric discharge machining, FESEM, Micro cracks, Response surface methodology

1 Introduction

In present age of technological development, EDM has become one of the most popular unconventional machining process. Due to contactless thermal erosion by EDM, it is widely used to machine variety of hard to cut conductive materials irrespective of their hardness. In the last few decades, EDM has gained more attention and has been widely used in various fields like the mould and die making industry, automobile industry, aviation industry and in surgical equipment[1]. In EDM process material is removed from workpiece due to the series of repetitive sparks developed between workpiece and tool electrode immersed in dielectric fluid. These series of repeated spark occur when a voltage of 80 - 320 V is applied between the electrodes at suitable electrode gap for sparking. This thermal energy generates a plasma channel between the electrodes with a temperature range of 8000 – 12000 ºC, which ultimately erodes the material by melting and vaporization from the vaporizing zone of the workpiece. Low machining efficiency and surface integrity are the prime concerns for the proper industrialization of the EDM process.Due to the unpredictable nature of the EDM process, researchers not only tried to improve the process performance by controlling various input parameters[2] but also applied various modifications by using different tool electrodes[3,4] and different EDM pulse generator[5]. A step further, various process alterations like workpiece ultrasonic vibration assisted EDM[6], dielectric ultrasonic vibration assisted EDM[7], tool ultrasonic vibration assisted EDM[8], workpiece rotary EDM[9], EDM with rotary tool[10] and near dry EDM[11] are also investigated and succeed to some extent to overcome the EDM challenges.But one of the process which get highest success towards EDM challenges, is powder mixed electric discharge machining (PMEDM). Jeswani[12]was the first who reported 60% improvement in MRR and 15% reduction in TWR by using Gr (4g/l concentration) PMEDMing of mild steel. .Fong and Chen[13] unfolded the powder characteristics and reported that the smallest particle size generates lower surface roughness and highest recast layer thickness.

*Corresponding author (E-mail: rajeshbajaj@jssaten.ac.in)

Kansal *et al.*[14] reported optimum setting of MRR, SR and TWR for Gr PMEDM of HCHCr die steel. Cogun *et al*.[15] reported that Gr PMEDMing of SAE 1040 steel shows remarkably higher MRR, lower SR, higher TWR and higher MH as compare to H_3BO_3 PMEDM due to better thermal conductivity of Gr powder. Peças and Henriques[16] reported lowest values of surface roughness, crater width, crater depth and recast layer thickness by using Si PMEDM. Bhattacharya*et al*.[17] revealed that Gr powder produces highest MH while Cu powder shows the smallest grain size on machined surface during the PMEDMing of various die steels. Mai *et al.*[18]reported 66% lower machining time and improved SR (0.09µm) by using CNT mixed EDM as compared to conventional EDM. Izman *et al*.[19]achieved higher MRR, lower SR and reduced recast layer thickness (RLT) as compare to conventional EDM by using MWCNT mixed EDM. Hu *etal.*[20]reported better surface finish, higher micro hardness and improved corrosion and wear resistance surface on SiCp/Al composite using Al PMEDM. Sari *et al.*[21]reported 154% higher MRR, 24% lower tool wear rate (TWR), 34% lower SR and 37% reduced RLT with MWCNT mixed EDM as compared to conventional EDM. H Kumar[22] achieved significant improvement in MRR and SF by using CNT mixed EDM as compared to conventional EDM. Marashi *et al*.[23] obtained 69% higher MRR and 35% reduced SR with Ti nano powder mixed EDM (NPMEDM) as compared to conventional EDM. Kumar *et al.*[24]reported improved MRR and lower SR with low cost Al_2O_3 NPMEDM as compared to conventional EDM. Wang and Yan[25] reported that higher MRR can be achieved in case of electric discharge blind hole drilling of Al_2O_3/6061Al composite using eccentric hole tool with the only concern of TWR. Guu and Hocheng[9] reported approximately twice time improvement in MRR and 50 % reduction in SR with workpiece rotation at 5000 rpm. Mohan *et al*.[26] reported that tool rotation plays a significant role to improve MRR and reduce SR in case of electric discharge machining of Al-SiC composite. Kuppan*et al*.[27] reported significant impact of tool rotation on enhancement MRR and Surface finish in deep hole drilling of Inconel 718. Govindan and Joshi[28] reported that tool rotation is one of the significant factor to enhance MRR in dry electric discharge drilling. Puthumana and Joshi[29] reported remarkable enhancement in MRR and decrement in TWR in dry EDM by using rotary slotted tool. Teimouri and Baseri[30,31] reported remarkable improvement in MRR and surface finish in case of magnetic field assisted rotary EDM due to better flushing of debris except high TWR and overcut were the only concern. All the above discussed research works prove that tool rotation has a significant impact on EDM machining process.Vishwakarma*et al*.[32] achieved approximately 2.5 times higher MRR with rotary EDM as compared to PMEDM of Al-SiC metal matrix composite. Baseri and Sadeghian[33] reported improved MRR, lower TWR and higher SF with TiO_2 NPMEDM using rotary tool as compared to conventional EDM. Based on the available literature survey, it was found that very little work has been reported on nano powder mixed rotary EDM (NPMREDM) and therefore present work investigate the machining performance of MWCNT mixed rotary EDM. Present study investigate the optimum setting of MRR and SR using GA available in MATLAB. Further multi –objective optimization (MOO) using GA, available in MATLAB is used for multiple response optimization.

2 Materials and Methods

2.1 Experimentation

The present investigation has been carried out on die sinking EDM (Make: J K MACHINES, Model: ZNC 25). An external rotary tool head has been developed by using DC motor, rotating chuck, timer belt drive and arduino chip to provide a range of rotational speed to the tool as shown in Fig.1. To

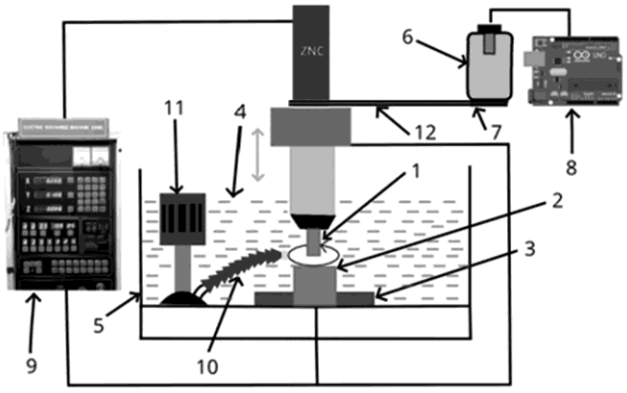

Fig. 1 — Schematic diagram of PMEDM set-up.

optimize the cost of the experiment powder use must be minimized. Therefore, a small tank made of acrylic material of size 30 X 22 X 13 cm^3 is used for experimental purpose which is filled by MWCNT mixed dielectric. A submersible pump attached with nozzles is also used to ensure proper flushing of the debris from the sparking zone.EN-31 die steel having chemical composition (C = 0.9–1.2%, Si = 0.1–0.35%, Mn = 0.3–0.75%, Cr = 1–1.6%, S and P each 0.025% (max.) and balance is ferrous) is used as a workpiece. The dimension of the workpiece were selected as 25 mm length, 25 mm width and 20 mm thickness for the present investigation. EN-31 die steel because of its high compressive strength, high hardness, and high abrasive resistance is widely used in bearings, spinning, punch and die industries. Cu rod with diameter 10 mm is used as a tool electrode and MWCNT (Length: 1-10 μm; OD: 5-20 nm; ID: 2-6 nm) mixed in EDM oil is used as a dielectric for the experimentation purpose. The present experimental study is carried out to achieve the optimum value of MRR and SR for MWCNT powder mixed rotary EDM using RSM and GA. Further, multi-objective optimization (MOO) available in MATLAB 2017a is used to achieve the common setting of input parameters for different optimum response values of MRR and SR. Further, the optimum values of MRR and SR for MWCNT mixed rotary EDM process is then compared with MWCNT mixed EDM, rotary EDM and conventional EDM, respectively. For this purpose, four independent input variables namely peak current (I_p), pulse on time (T_{on}), pulse off time (T_{off}) and powder concentration (P_c) are selected, based on Ishikawa cause effect diagram as shown in Fig.2. The range of input parameters was selected based on pilot test (varying one variable and keeping other constant) and are given in Table 1. Further, the result of pilot test showcased in Fig.3, which demonstrate the effect of individual parameter on MRR and SR.

Optimization of MRR and SR was the prime objective during the present investigation. Therefore, measurement of MRR were done by measuring the difference between the weight of workpiece before and after the machining. Further this difference in weight of workpiece before and after machining is converted into volumetric loss as:

$$MRR(mm^3/min) = \frac{W_b - W_a}{\rho \times t} \times 1000 \quad \ldots (1)$$

Where,
W_b = weight of workpiece before machining in gm.
W_a = weight of workpiece after machining in gm,
ρ = density of workpiece material (g/cm^3)
t = machining time (min)

Table 1 — Selected range of input parameters for optimization purpose.

Factor Symbol	Parameter	Symbol	Levels		
			Low (-1)	Medium (0)	High (+1)
I_p	Peak current (Ampere)	I_p	3	5	7
T_{on}	Pulse on time (μs)	T_{on}	100	150	200
T_{off}	Pulse off time (μs)	T_{off}	40	70	100
P_c	Powder concentration (g/l)	P_c	1	2	3
T_r	Tool rotation (rpm)			1200	
	Polarity			Negative	

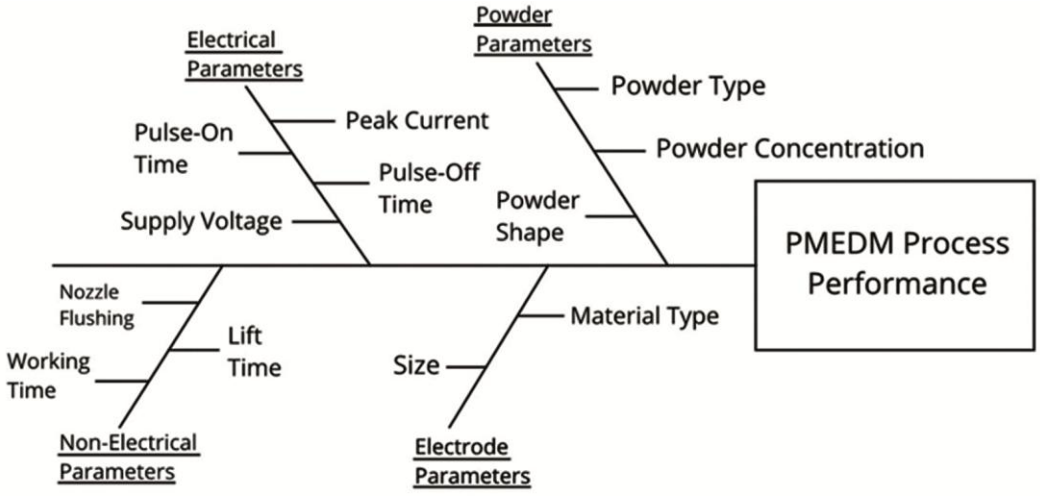

Fig.2 — The Ishikawa cause-effect diagram for PMEDM process.

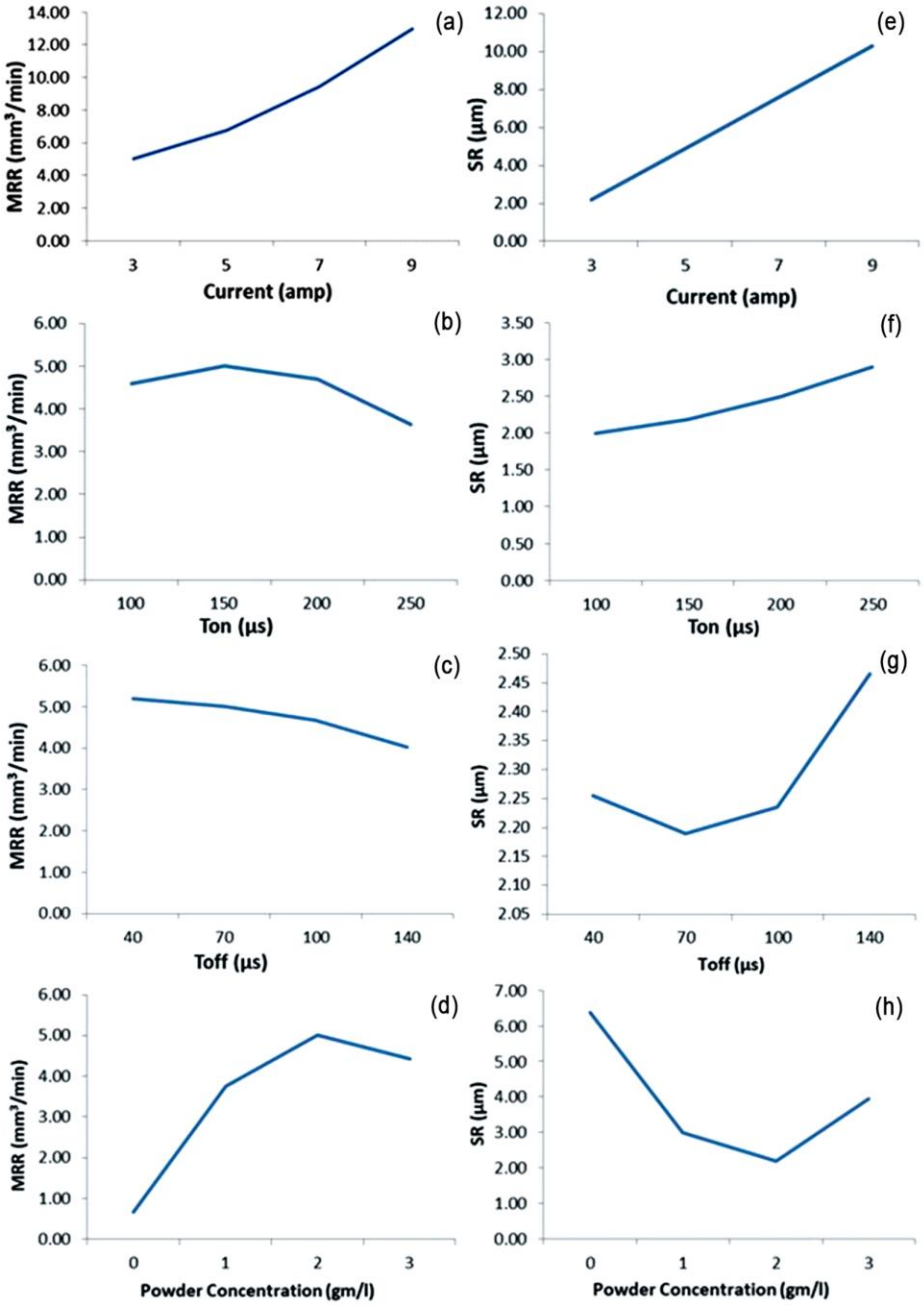

Fig. 3 — Effect of (a) I_p on MRR, (b) T_{on} on MRR, (c) T_{off} on MRR, (d) P_c on MRR, (e) I_p on SR, (f) T_{on} on SR, (g) T_{off} on SR and (h) P_c on SR.

In present investigation surface roughness is measured in term of R_a,which is arithmetic mean of peak and valleys of the surface irregularities measured microscopically. To measure the R_a value after each experiment MITUTOYO surface tester (model: SJ 310) is used throughout the experimentation.

2.2 Response Surface Modeling

RSM is a well-known designing as well as optimization technique for multi interacting process parameters. This technique is not only used to investigate the effect of individual input parameters but also used to examine the effect of interaction of input parameters. In RSM performance parameters and input parameters are connected as[34]:

$$y = f(x_1, x_2, x_3 \ldots\ldots\ldots x_p) \quad \ldots (2)$$

where,x_1 , x_2 , x_3 are the input process parameters and y is the output performance parameter. Generally

a quadratic model of input parameters is used for the modeling of fitness function which is as follows:

$$y = c_0 + \sum_{i=1}^{p} c_{ii} x_i^2 \sum i \sum j c_{ij} x_i x_j \quad \ldots (3)$$

where, c_0 represent constant and all other $c's$ are the coefficient.

2.3 Genetic Algorithm

Genetic algorithm (GA) is a unique technique to provide solution for both constrained and unconstrained optimization problems by generating a random initial population comprising of set of input parameters. The fitness function, which is generally used to transform the objective function value into a measure of relative fitness[35] thus:

$$F(x) = g(f(x)) \quad \ldots (4)$$

where, f is the objective function, g transform the value of objective function to a positive number and F shows the resulting relative fitness. The individual fitness, $F(x_i)$, of each individual is calculated as the individual's raw performance $f(x_i)$, relative to the whole population i.e.

$$F(x_i) = \frac{f(x_i)}{\sum_{i=1}^{N_{ind}} f(x_i)} \quad \ldots (5)$$

where, N_{ind} is the size of population and x_i is the phenotypic value of individual i.

The values of important GA parameters for entire process are chosen as follows: population size = 50, cross over fraction = 0.8, mutation rate = 0.01 and number of generations = 100.

A quadratic model for MRR and SR was developed by using RSM (Box-Behnken technique) available in Design Expert 6 Software. Total 30 numbers of experiments were performed thrice to achieve the average value of MRR and SR against each experiment as shown in Table 2. Further these results of MRR and SR and are used to generate quadratic model of MRR and SR generated by Design Expert 6 software as shown in Eq. (6) and Eq. (7).

Table 2 — Design of experimental matrix and corresponding response value against each setting.

Run No.	Process Parameters				MRR (mm^3/min)				SR (μm)			
	I_p(A)	T_{on}(μs)	T_{off}(μs)	P_c(g/l)	1	2	3	Average	1	2	3	Average
1	5	150	40	3	6.16	6.09	6.08	6.11	6.71	6.64	6.63	6.66
2	7	200	70	2	9.33	9.32	9.19	9.28	7.87	7.92	7.88	7.89
3	7	100	70	2	8.56	8.59	8.68	8.61	7.32	7.33	7.25	7.3
4	5	150	70	2	6.67	6.65	6.75	6.69	4.91	4.89	4.84	4.88
5	5	150	70	2	6.79	6.82	6.73	6.78	4.83	4.88	4.84	4.85
6	5	150	40	1	5.34	5.42	5.35	5.37	5.88	5.83	5.87	5.86
7	5	150	100	3	5.91	5.85	5.82	5.86	6.61	6.63	6.71	6.65
8	5	150	100	1	5.17	5.12	5.13	5.14	5.89	5.87	5.79	5.85
9	3	100	70	2	4.26	4.35	4.32	4.31	2.08	2.13	2.06	2.09
10	3	200	70	2	4.67	4.63	4.56	4.62	2.61	2.68	2.66	2.65
11	7	150	70	3	9.13	9.16	9.04	9.11	9.08	9.11	9.17	9.12
12	3	150	70	1	3.97	3.96	3.89	3.94	2.82	2.89	2.87	2.86
13	5	150	70	2	6.76	6.84	6.77	6.79	4.93	4.89	4.82	4.88
14	7	150	70	1	8.19	8.24	8.11	8.18	8.61	8.54	8.53	8.56
15	5	200	40	2	6.85	6.78	6.83	6.82	5.07	5.12	5.08	5.09
16	3	150	70	3	4.68	4.72	4.73	4.71	3.78	3.72	3.69	3.73
17	5	200	100	2	6.56	6.51	6.55	6.54	5.11	5.08	4.99	5.06
18	5	150	70	2	6.71	6.64	6.69	6.68	4.81	4.84	4.75	4.80
19	5	100	40	2	6.33	6.43	6.41	6.39	4.66	4.73	4.68	4.69
20	5	100	100	2	6.26	6.31	6.27	6.28	4.65	4.67	4.72	4.68
21	5	200	70	3	5.76	5.83	5.84	5.81	6.96	6.94	6.84	6.92
22	5	200	70	1	5.07	5.04	4.95	5.02	6.11	6.16	6.12	6.13
23	7	150	100	2	9.27	9.24	9.15	9.22	7.64	7.69	7.62	7.65
24	5	150	70	2	6.75	6.82	6.77	6.78	4.93	4.9	4.84	4.89
25	5	100	70	3	5.61	5.69	5.59	5.63	6.47	6.52	6.48	6.49
26	3	150	40	2	5.23	5.19	5.09	5.17	2.29	2.36	2.28	2.31
27	3	150	100	2	4.63	4.59	4.52	4.58	2.33	2.31	2.23	2.29
28	7	150	40	2	9.36	9.29	9.28	9.31	7.69	7.68	7.61	7.66
29	5	100	70	1	5.09	5.16	5.11	5.12	5.42	5.51	5.45	5.46
30	5	150	70	2	6.75	6.82	6.77	6.78	4.85	4.94	4.88	4.89

$$MRR = -2.46256 - 0.36646*I_p + 0.04180*T_{on} + 1.26852E\text{-}003*T_{off} + 3.76167*P_c + 0.11448*I_p^2 - 1.47333E\text{-}004*T_{on}^2 - 8.14815E\text{-}005*T_{off}^2 - 0.92208*P_c^2 + 9.00000E\text{-}004*I_p*T_{on} + 2.08333E\text{-}003*I_p*T_{off} + 0.020000*I_p*P_c - 2.83333E\text{-}005*T_{on}*T_{off} + 1.40000E\text{-}003*T_{on}*P_c - 1.66667E\text{-}004*T_{off}*P_c \quad \ldots(6)$$

$$SR = +1.89882 + 1.37583*I_p + 7.08333E\text{-}004*T_{on} - 8.51389E\text{-}003*T_{off} - 4.36208*P_c + 3.12500E\text{-}003*I_p^2 + 2.20000E\text{-}005*T_{on}^2 + 6.11111E\text{-}005*T_{off}^2 + 1.28500*P_c^2 + 7.50000E\text{-}005*I_p*T_{on} + 4.1666E\text{-}005*I_p*T_{off} - 0.038750*I_p*P_c - 3.33333E\text{-}006*T_{on}*T_{off} - 1.20000E\text{-}003*T_{on}*P_c + 1.06917E\text{-}016*T_{off}*P_c \quad \ldots(7)$$

The acceptability of the model is required for the analysis of data and for this purpose goodness of fit of the model is required, which includes the checking of model significant test, coefficient test, model coefficient test and lack of fitness test[36]. ANOVA is carried out to check the overall acceptability of MRR and SR models.These response models are further used to optimize for individual response and multiple response by using GA in MATLAB R2017a.

2.4 Analysis of MRR Model

Quadratic model for MRR is further investigated by using ANOVA at 95% confidence level to check the Acceptability of the model. The ANOVA result for MRR is shown in Table 3. MRR model shows an excellent relationship between input parameters and response (MRR) since the value of $R^2$and adjusted R^2 are 99.61% and 99.19% which provides best justification for co-relation input parameters and response. Signal to noise ratio is associated with adequate precision and if this term has a value more than 4, the model is fit for optimization. The associated p - value for the MRR model is significantly less than 5% (< 0.05) which indicated that the model is statically significant [36]. Further, it can be observed from the ANOVA model that lack of fit is non- significant which also support the acceptance of the model. The term A (I_p), B (T_{on}), C (T_{off}), D (P_c), A^2, B^2, D^2 and AD appear as significant variables while the remaining variables and their interactions are non-significant. Further, Fig. 4(a)

Table 3 — ANOVA table for MRR model.

Source	Sum of Squares	DF	Mean Square	F Value	Prob> F	
Block	0.39	2	0.19			
Model	69.18	14	4.94	237.63	< 0.0001	significant
A	57.99	1	57.99	2788.61	< 0.0001	
B	0.26	1	0.26	12.27	0.0039	
C	0.20	1	0.20	9.63	0.0084	
D	1.66	1	1.66	79.71	< 0.0001	
A2	1.44	1	1.44	69.14	< 0.0001	
B2	0.93	1	0.93	44.73	< 0.0001	
C2	0.037	1	0.037	1.77	0.2059	
D2	5.83	1	5.83	280.35	< 0.0001	
AB	0.032	1	0.032	1.56	0.2340	
AC	0.063	1	0.063	3.01	0.1066	
AD	6.400E-03	1	6.400E-03	0.31	0.5885	
BC	7.225E-03	1	7.225E-03	0.35	0.5657	
BD	0.020	1	0.020	0.94	0.3494	
CD	1.00E-04	1	1.000E-04	4.809E-03	0.9458	
Residual	0.27	13	0.021			
Lack of Fit	0.26	10	0.026	7.73	0.0595	not significant
Pure Error	0.010	3	3.367E-03			
Cor Total	69.84	29				
Std. Dev.	= 0.14			R-Squared		= 0.9961
Mean	= 6.39			Adj. R-Squared		= 0.9919
C.V.	= 2.26			Pred R-Squared		= 0.9774
PRESS	= 1.57			Adeq Precision		= 49.553

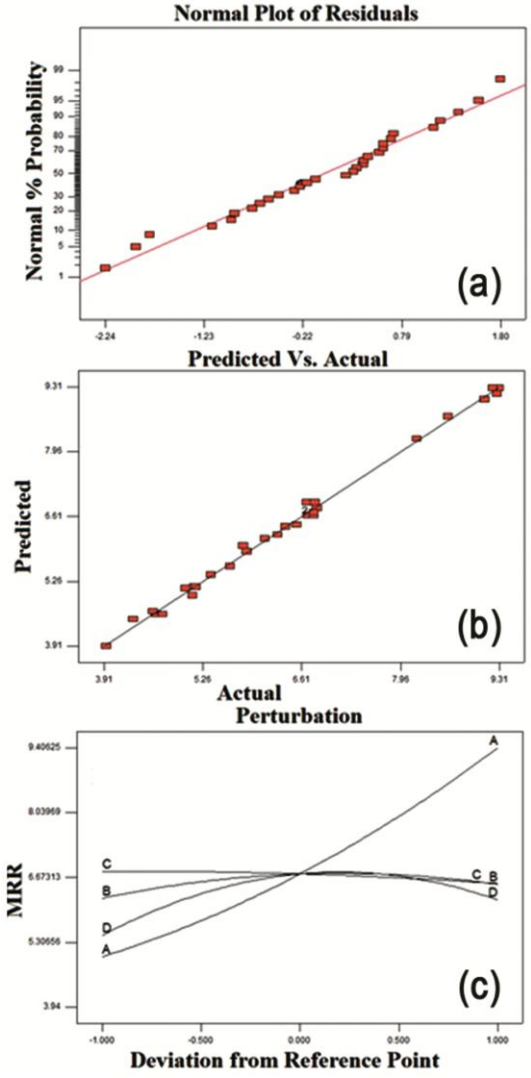

Fig. 4 — (a) Normal probability plots of residuals for MRR, (b) Actual versus predicted response for MRR and (c) Perturbation graph for MRR.

shows normal plots of residuals for MRR and it is clear from the figure that most of the plots are lying on or along the straight line which is a clear cut indication of uniform scattering of errors. Figure 4(b) shows the excellent closeness between actual values and predicted values of MRR, which indicate that regression model is well suited for the actual values of MRR. Finally, Fig. 4(c) shows the perturbation plot for MRR which shows the effect of each individual parameter on MRR while keeping other parameters constant

2.5 Optimization of MRR Using GA

The mathematical model for MRR is used as an input function for GA without any constraint. MATLAB response for predicted optimum value of MRR appear as 9.50 mm^3/min, which is shown in Fig. 5(a) and corresponding input parameters setting are shown in Fig. 5(b). It can be observed from Fig. 5 (a) that in initial population of the generation, the best and average value of MRR varies significantly. But as the iterations proceed, the best and average value difference become non-significant. Further, it becomes very difficult to reduce the different between best and average value of MRR as the iterations proceed.

2.6Analysis of Surface Roughness Model

ANOVA analysis for SR model is shown in Table 4, which shows that proposed model exhibit excellent correlation between input parameters and response (SR). The value of $R^2$and adjusted R^2 are 99.24% and 98.54% respectively, which shows excellent correlation between input parameters and output response (SR). Adequate Precision which is linked with signal to noise ratio shows value 47.777, which is more than 4 and makes the model quite fit for optimization. The associated p - value for the SR model is significantly less than 5% (< 0.05) which shows that model is accepted as a statically significant model[36]. Further Fig. 6(a) shows the normal plots of residuals for SR. It is clear from the figure that most of the plots lie on or along the straight line which is a clear cut indication of uniform scattering of errors. Figure 6(b) shows the excellent closeness between actual values and predicted values of SR, which indicate that regression model is well suited for the actual values of SR. Finally, Fig. 6(c) shows the perturbation plot for SR which shows the effect of each individual parameter on SR while keeping other parameters constant.

Table 4 — ANOVA table for SR model.

Source	Sum of Squares	DF	Mean Square	F Value	Prob> F	
Block	0.098	2	0.049			
Model	101.11	14	7.22	875.45	< 0.0001	significant
A	86.67	1	86.67	10506.01	< 0.0001	
B	0.77	1	0.77	92.74	< 0.0001	
C	6.750E-04	1	6.750E-004	0.082	0.7794	
D	1.96	1	1.96	237.61	< 0.0001	
A2	1.071E-003	1	1.071E-003	0.13	0.7244	
B2	0.021	1	0.021	2.51	0.1368	
C2	0.021	1	0.021	2.51	0.1368	
D2	11.32	1	11.32	1372.49	< 0.0001	
AB	2.250E-004	1	2.250E-004	0.027	0.8714	
AC	2.500E-005	1	2.500E-005	3.03E-03	0.9569	
AD	0.024	1	0.024	2.91	0.1117	
BC	1.000E-04	1	1.000E-004	0.012	0.9140	
BD	0.014	1	0.014	1.75	0.2092	
CD	0.000	1	0.000	0	1.0000	
Residual	0.11	13	8.250E-003			
Lack of Fit	0.10	10	0.010	8.51	0.0522	not significant
Pure Error	3.650E-003	3	1.217E-003			
Cor Total	101.32	29				
Std. Dev.	= 0.091			R-Squared		= 0.9989
Mean	= 5.43			Adj. R-Squared		= 0.9978
C.V.	= 1.67			Pred R-Squared		= 0.9922
PRESS	= 0.79			Adeq Precision		= 103.194

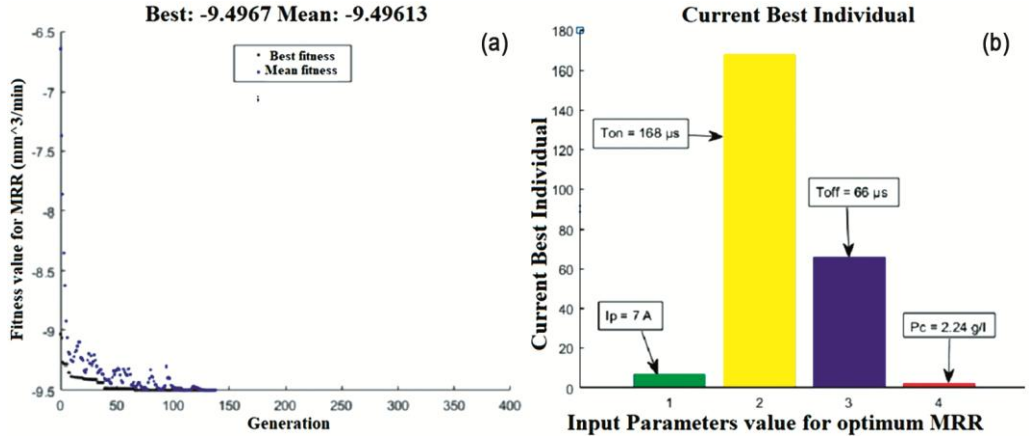

Fig.5 — MATLAB response for (a) MRR fitness curve and (b) Optimum MRR input setting.

2.7 Optimization of SR Using GA

The mathematical model for the minimization of SR is used as an input function for GA to optimize it. MATLAB generated fitness curve Fig. 7(a) shows predicted minimum value of SR (Ra = 1.96 μm) and Fig. 7(b) shows the corresponding input parameters setting. Similar to the MRR fitness curve, SR fitness curve is also converging and best and average values of SR are approximately coinciding as the iterations move forward.

2.8 Multi-objective Optimization with Genetic Algorithm

In multi-objective optimization with GA, a mathematical model for MRR and SR are used to develop a common objective function. MATLAB response for MOO appears as Pareto table (Table 5) and Pareto front (Fig. 8). Pareto table shows different input values and corresponding optimal values of MRR and SR and Pareto front shows the graphical representation of these optimum values of MRR and SR. It is clear from the Pareto front and Pareto table that if higher MRR is required than SR will also be high and if low SR is required than MRR will also be low. Therefore a compromised value of MRR and SR can be selected by using corresponding input parameters setting.

3 Results and Discussion

3.1 Analysis of MRR

The predicted and experimental value of MRR for MWCNT mixed rotary EDM are 9.50 mm^3/min and

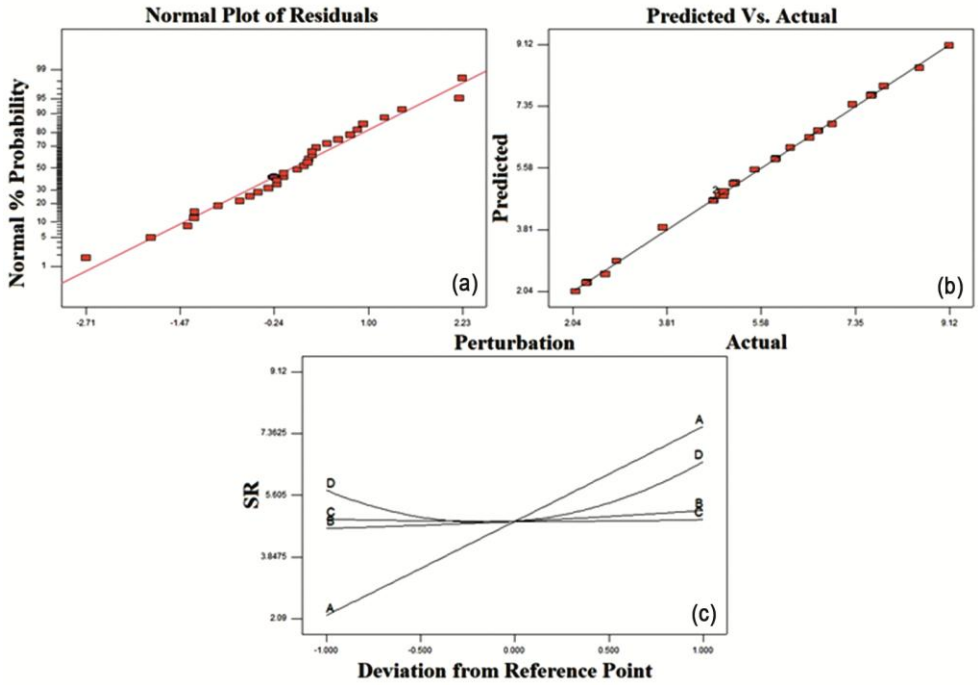

Fig. 6 — (a) Normal probability plots of residuals for SR, (b) Actual versus predicted response for SR and (c) Perturbation graph for SR.

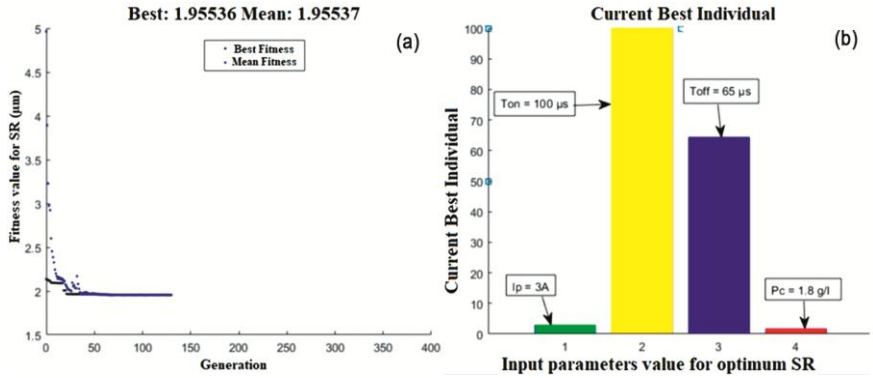

Fig.7 — MATLAB response for (a) SR fitness curve and (b) Optimum SR input setting.

9.72 mm^3/min respectively at optimum input parameters setting. Result shows that experimental value of MRR at optimal setting are very close to predicted value of MRR and showing 2.31 % error between them. Experiments were also carried out for conventional EDM, conventional rotary EDM and PMEDM to find the optimum MRR for respective processes. MRR results for conventional EDM, REDM, PMEDM and RPMEDM at corresponding optimum setting is shown in Table 6 and also shown in Fig.9 (a). All these results indicates that REDM shows approximately 22.86% higher MRR than conventional EDM while PMEDM shows approximately 37.14% and 11.63% higher MRR than conventional EDM, respectively and REDM and finally PMREDM shows approximately 46.17%, 18.9% and 6.58% higher MRR than conventional EDM, REDM and PMEDM respectively. Highest value of MRR for PMREDM occurs due to presence of MWCNT in dielectric which not only increases the discharge gap between two electrodes but also increases the discharge transitivity and tool rotation provides extra support towards the enhancement of MRR due to better flushing. Further, rotary EDM shows better MRR than conventional EDM because rotary action of the tool provide extra support to the debris to exit and minimizes the chances of re-attaching these debris from machining area.Highest value of MRR for MWCNT mixed rotary EDM occurs at highest I_p, medium T_{on}, low $T_{off}$and medium P_c. Since high I_p produces high pulse energy and

Table 5 — MATLAB generated Pareto table for MOO versus input parameters.

SNo	Response		Input parameters			
	MRR (mm^3/min)	SR (µm)	IP (A)	T_{on} (µs)	T_{off} (µs)	P_c (g/l)
1	-5.31	3.06	3.79	116.05	61.59	1.81
2	-9.08	7.41	6.91	123.88	65.66	2.16
3	-8.93	7.23	6.72	136.50	71.63	2.18
4	-7.68	5.93	5.82	137.47	67.55	2.05
5	-4.67	1.98	3.00	107.00	57.54	1.79
6	-7.24	5.48	5.49	132.51	67.70	2.08
7	-4.90	2.17	3.10	120.43	67.92	1.92
8	-5.06	2.57	3.42	117.67	61.53	1.82
9	-9.43	7.68	7.00	146.15	77.02	2.22
10	-7.37	5.62	5.62	131.78	67.37	2.01
11	-5.61	3.42	4.03	121.49	68.76	1.96
12	-5.79	3.61	4.15	126.81	64.95	1.99
13	-6.41	4.43	4.65	141.99	63.62	2.12
14	-7.04	5.29	5.28	142.74	75.49	2.14
15	-8.14	6.46	6.24	127.62	68.21	2.08
16	-6.23	4.22	5.58	133.58	68.61	2.00
17	-6.80	4.98	5.12	131.15	68.60	2.07
18	-8.49	6.82	6.41	138.43	76.43	2.19
19	-5.91	3.85	4.34	128.89	68.55	1.87
20	-9.40	7.67	6.98	146.15	77.03	2.23
21	-5.22	2.67	3.46	125.50	62.11	1.92
22	-7.48	5.74	5.65	137.16	69.82	2.11

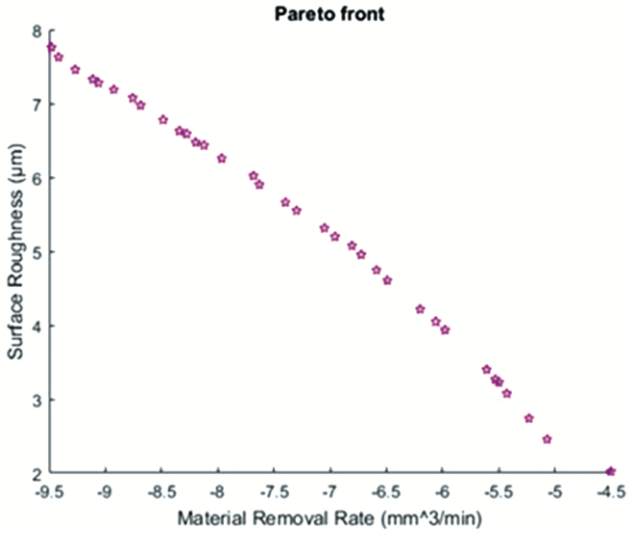

Fig.8 — MATLAB generated Pareto front graph for MRR and SR.

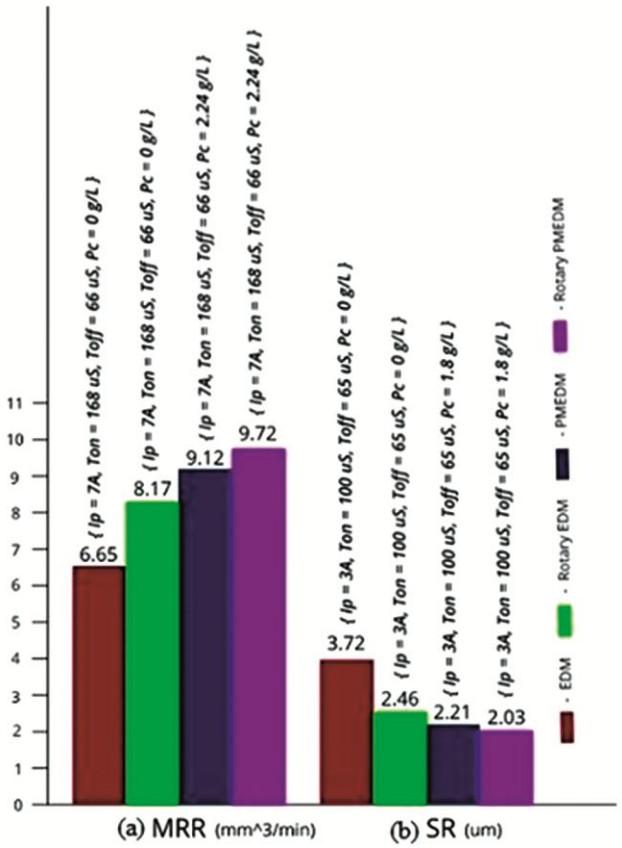

Fig. 9 — (a) MRR and (b) SR comparison of EDM, rotary EDM and powder mixed rotary EDM (PMREDM) at corresponding optimum setting.

Table 6 — MRR and SR results for PMREDM, PMEDM, REDM and EDM processes.

S. No.	Process	Response Setting	Response value
1	PMREDM	MRR (I_p = 7A, T_{on} = 168µs, T_{off} = 66µs, P_c = 2.24g/l) & N = 1200RPM	9.72(mm^3/min)
		SR (I_p = 3A, T_{on} = 100µs, T_{off} = 65µs, P_c = 1.8g/l) & N = 1200RPM	2.03(µm)
2	PMEDM	MRR (I_p = 7A, T_{on} = 168µs, T_{off} = 66µs, P_c = 2.24g/l) & N = 0RPM	9.12 (mm^3/min)
		SR (I_p = 3, T_{on} = 100, T_{off} = 65, P_c = 1.8) & N = 0	2.21(µm)
3	REDM	MRR (I_p = 7A, T_{on} = 168µs, T_{off} = 66µs) & N = 1200RPM	8.17(mm^3/min)
		SR (I_p = 3A, T_{on} = 100µs, T_{off} = 65µs) & N = 1200RPM	2.46(µm)
4	EDM	MRR (I_p = 7A, T_{on} = 168µs, T_{off} = 66µs)	6.65(mm^3/min)
		SR ((I_p = 3A, T_{on} = 100µs, T_{off} = 65µs)	3.72(µm)

therefore deeper size craters are produced, which finally leads to higher MRR. Further as the T_{on} increases, MRR increases but as it goes beyond a certain value it produces more debris and lees time for them to exit from machining area which ultimately leads to resolidification of debris onto machined area and reducing the MRR. Increasing T_{off} directly reduces the MRR. Finally, highest MRR achieved at approximately middle level of P_c because as the P_c increases, more chain formation and multiple sparks occurs at different places but increasing P_c beyond a certain level decreases MRR due to high discharge turbulence.

3.2 Analysis of Surface Roughness

The predicted and experimental value of SR for MWCNT mixed rotary EDM are 1.96 µm and 2.03 µm respectively at optimum input parameters setting. Validation result shows that predicted and experimental value of SR are very close to each other with an accepted error of 3.57%. Experiments were also carried out for conventional EDM, conventional rotary EDM and PMREDM to find the optimum value of SR for respective processes. SR result for conventional EDM, REDM, PMEDM and PMREDM at corresponding optimum setting is shown in Table 6 and also shown in Fig.9 (b). All these results indicates that REDM shows approximately 33.87% lower SR than conventional EDM while PMEDM shows approximately 40.59% and 10.16% lower SR than conventional EDM and REDM, respectively and finally PMREDM shows approximately 45.43%, 17.48% and 8.15% lower SR than conventional EDM, REDM and PMEDM, respectively. Lowest value of SR is achieved at low I_p, low T_{on}, and medium level of P_c while T_{off} appears as a non-significant factor. Low I_p produces low pulse energy resulting in small and shallow craters on the workpiece which ultimately leads to better surface quality. Increasing T_{on} produces more machined particles and more chances to adhere on the workpiece therefore increasing the SR. Further increasing P_c beyond the optimum value increases SR since high P_c increases discharge turbulence and produces uneven machined surface.

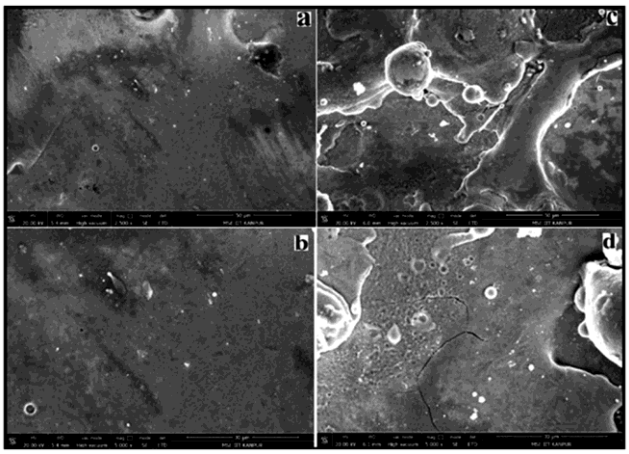

Fig. 10 — (a, b) FESEM images of MWCNT mixed rotary EDMed surfaces and (c, d) EDM surfaces.

3.3 Surface Topography

Surface topography plays an important role for the components which are very costly and working under high stress conditions and the safety of whole system mostly depends on these components. EDM is one of the most important unconventional machining process used to develop many such crucial parts in mold and die making industries, automobile and aviation industries. Therefore along with surface quality of the machined part, topography of the surface was also examined for MWCNT mixed rotary EDM and conventional EDM. The EN-31 surface machined with MWCNT mixed rotary EDM at input parameters setting (I_p = 3A, T_{on} = 100 µs, T_{off} = 65 µs, P_c = 1.8 g/l) are examined for surface topography using FESEM. At low magnification, MWCNT mixed rotary EDM shows superior surface with smaller resolidified layer on the machined surface (Fig. 10a) while surface machined through EDM process shows uneven surface with thick resolidified layer on the machined surface (Fig. 10c). Further, at high magnification very few

micro cracks appears on the MWCNT mixed rotary EDM (Fig. 10b) while EDM machined surface shows bigger micro crack along with micro holes which are clearly visible in Fig. 10d. MWCNT mixed rotary EDM shows superior surface topographical properties because of MWCNT powder mixed in the dielectric medium. Adding MWCNT powder not only increases the number of spark in the machining zone but also reduces the energy associated with each spark. Therefore less amount of thermal energy is transferred in the machining area. Further, the high thermal conductivity of MWCNT particles mixed in EDM dielectric enhances the heat transfer capability of plasma channel developed and therefore reducing the heat flow rate towards the workpiece. Therefore reducing the thermal stresses and solidifying shrinkages. Further, increased spark gap and rotary action of tool electrode which provide better flushing condition and ultimately providing a major reason for better surface quality than conventional EDM.

4 Conclusions

Performance enhancement of EN-31die steel using MWCNT mixed rotary EDM results in the following conclusion:

(i) MWCNT mixed rotary EDM shows maximum value of MRR (9.72 mm^3/min) at I_p = 7A, T_{on} = 168 µs, T_{off} = 66 µs and P_c = 2.24 g/l, which is very close to the predicted value of MRR (9.50 mm^3/min). Further, RPMEDM shows approximately 46.17 %, 18.90 % and 6.58 % higher than EDM, REDM and PMEDM respectively.

(ii) MWCNT mixed rotary EDM shows lowest vale of SR (2.03 µm) at I_p = 3A, T_{on} = 100 µs, T_{off} = 65 µs and P_c = 1.8 g/l, which very close to predicted SR value (1.96 µm). Further, PMREDM shows approximately 45.43 %, 17.48 % and 8.15 % lower SR than conventional EDM, REDM and PMEDM respectively.

(iii) With the help of MOO result shown in Pareto Table 5, input parameter can be selected against required optimum value of. MRR and SR.

(iv) FESEM analysis of MWCNT mixed rotary EDM shows superior surface topography as compared to conventional EDM.

References

1 Ho K H & Newman S T, *Int J Mach Tools Manuf*, 43 (2003) 1287.

2 Panda D K & Bhoi R K, *Mater Manuf Process*, 21 (2006) 853.

3 Karunakaran K & Chandrasekaran M, *Investigation of Machine-ability of Inconel 800 in EDM with Coated Electrode*,International Conference on Emerging Trends in Engineering Research, Chennai, India (2017).

4 Ndaliman MB, Khan AA, Ali M Y & Hambiyah MM, *Modelling the surface roughness behaviour of an EDMed workpiece with different tool electrodes using DoE*, 5th International Conference on Mechatronics, Kuala Lumpur, Malaysia (2013).

5 Muthuramalingam T & Mohan B, *Int J Manuf Technol Manag*, 27 (2013) 101.

6 Mishra V & Pandey P M, *Mater Manuf Process*, 33 (2018) 1.

7 Jafferson J, Hariharan P & Ram Kumar J, *Mater Manuf Process*, 29 (2014) 357.

8 Huang H, Zhang H, Zhou L & Zheng H Y, *J Micromech Microeng*, 13 (2003) 693.

9 Guu Y & Hocheng H, *Mater Manuf Process*, 16 (2001) 91.

10 Baseri H, Aliakbari E & Alinejad G, *Int J Mach Mach Mater*, 11 (2012) 297

11 Dhakar K, Pundir H, Dvivedi A & Kumar P, *Int J Mach Mach Mater*, 17 (2015) 127.

12 Jeswani M, *Wear*, 70 (1981) 133.

13 Yih-Fong T & Fu-Chen C, *J Mater Process Technol*, 170 (2005) 385.

14 Kansal H, Singh S, & Kumar P, *Int J Manuf Technol Manag*, 7 (2005) 329.

15 Cogun C, Özerkan B & Karacay T, *Proc Inst Mech Eng, Part B: J Eng Manuf*, 220 (2006) 1035.

16 Peças P & Henriques E, *Int J Adv Manuf Technol*, 37 (2008) 1120.

17 Bhattacharya A & Batish A, *Proc Inst Mech Eng, Part B: J Eng Manuf*, 226 (2012) 1192.

18 Mai C, Hocheng H & Huang S, *Int J Adv Manuf Technol*, 59 (2012) 111.

19 Izman S, Ghodsiyeh D, Hamed T, Rosliza R & Rezazadeh M, *In Adv Mater Res*, 463 (2012) 1445.

20 Hu F Q, Cao F Y, Song B Y, Hou P J, Zhang Y, Chen K & Wei J Q, *Procedia CIRP*, 6 (2013) 101.

21 Sari M M, Noordin M, & Brusa E, *IntJAdvManufTechnol*, 68 (2013) 1095.

22 Kumar H, *Int J Adv Manuf Technol*, 76 (2015) 105.

23 Marashi H, Sarhan A A & Hamdi M, *App Surf Sci*, 357 (2015) 892.

24 Kumar A, Mandal A, Dixit A R & Das A K, *Mater Manuf Process*, 33 (2017) 986.

25 Wang C C& Yan B H, *J Mater Process Technol*, 102 (2000) 90.

26 Mohan B, Rajadurai A & Satyanarayana K, *J Mater Process Technol*, 124 (2002) 297.

27 Kuppan P, Rajadurai A, & Narayanan S, *Int J Adv Manuf Technol*, 38(2008) 74.

28 Govindan P & Joshi S S, *Int J Mach Tools Manuf*, 50 (2010) 431.

29 Puthumana G & Joshi S S, *Int J Pr Eng Manuf*, 12 (2011) 957.

30 Teimouri R&Baseri H, *J Manuf Process*, 14 (2012) 316.

31 Teimouri R & Baseri H, *Adv Tribol*, 2012 (2012) 1.

32 Vishwakarma U K, Dvivedi A, &Kumar P, *Int J Mach Mach Mater*, 16(2014)113.

33 Baseri H & Sadeghian S, *Int J Adv Manuf Technol*, 83 (2016) 519.

34 Montgomery D C, **Design and Analysis of Experiments, (**John Wiley & Sons), ISBN: 9781119320937, 2017.

35 De Jong K A, *Analysis of the behavior of a class of genetic adaptive systems*, in *Dept. of Computer and Communication Sciences*. Ph.D. Thesis, University of Michigan, Ann Arbor, United States, 1975.

36 Montgomery D C, Peck E A, Vining G G, **Introduction to Linear Regression Analysis**, (John Wiley & Sons) ISBN: 9780470542811, 2012.